

Supporting information

Redox behavior of potassium doped and transition metal co-doped $\text{Ce}_{0.75}\text{Zr}_{0.25}\text{O}_2$ for thermochemical $\text{H}_2\text{O}/\text{CO}_2$ splitting

Maria Portarapillo[†], Gianluca Landi^{‡}, Giuseppina Luciani^{†*}, Claudio Imparato[†], Giuseppe
Vitiello^{†,‡}, Fabio A. Deorsola[§], Antonio Aronne[†], Almerinda Di Benedetto[†]*

[†] Dipartimento di Ingegneria Chimica, dei Materiali e della Produzione Industriale, Univ. of Naples
Federico II, P.le Tecchio 80, 80125, Naples, Italy.

[‡] Institute of Sciences and Technologies for Sustainable Energy and Mobility, CNR, P.le Tecchio
80, 80125, Naples, Italy.

[§] CSGI, Center for Colloids and Surface Science, 50019, Florence, Italy

[§] Department of Applied Science and Technology, Politecnico di Torino, corso Duca degli Abruzzi
24, 10129 Turin, Italy

*corresponding author: gianluca.landi@stems.cnr.it & luciani@unina.it

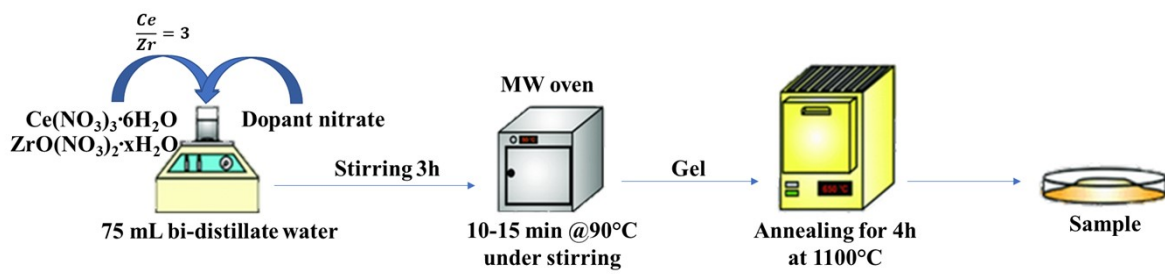


Figure S1. Co-precipitation synthesis steps of the doped ceria materials.

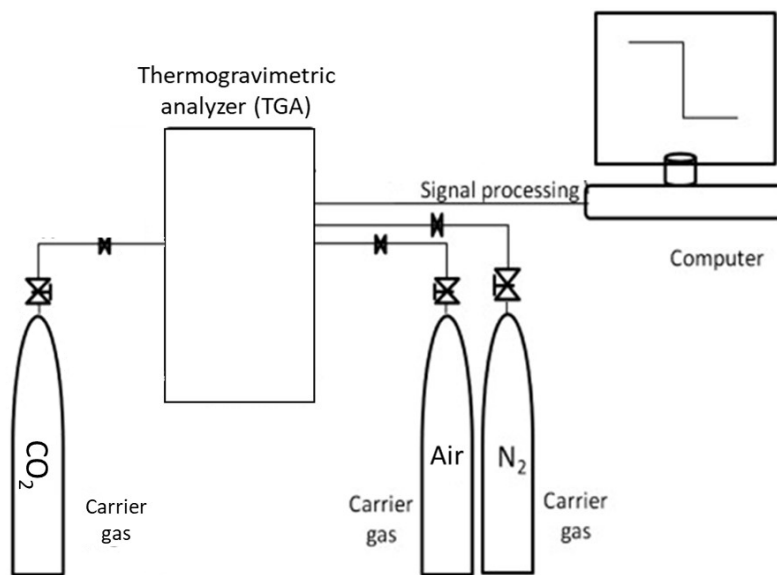


Figure S2. Schematic of the TGA apparatus.

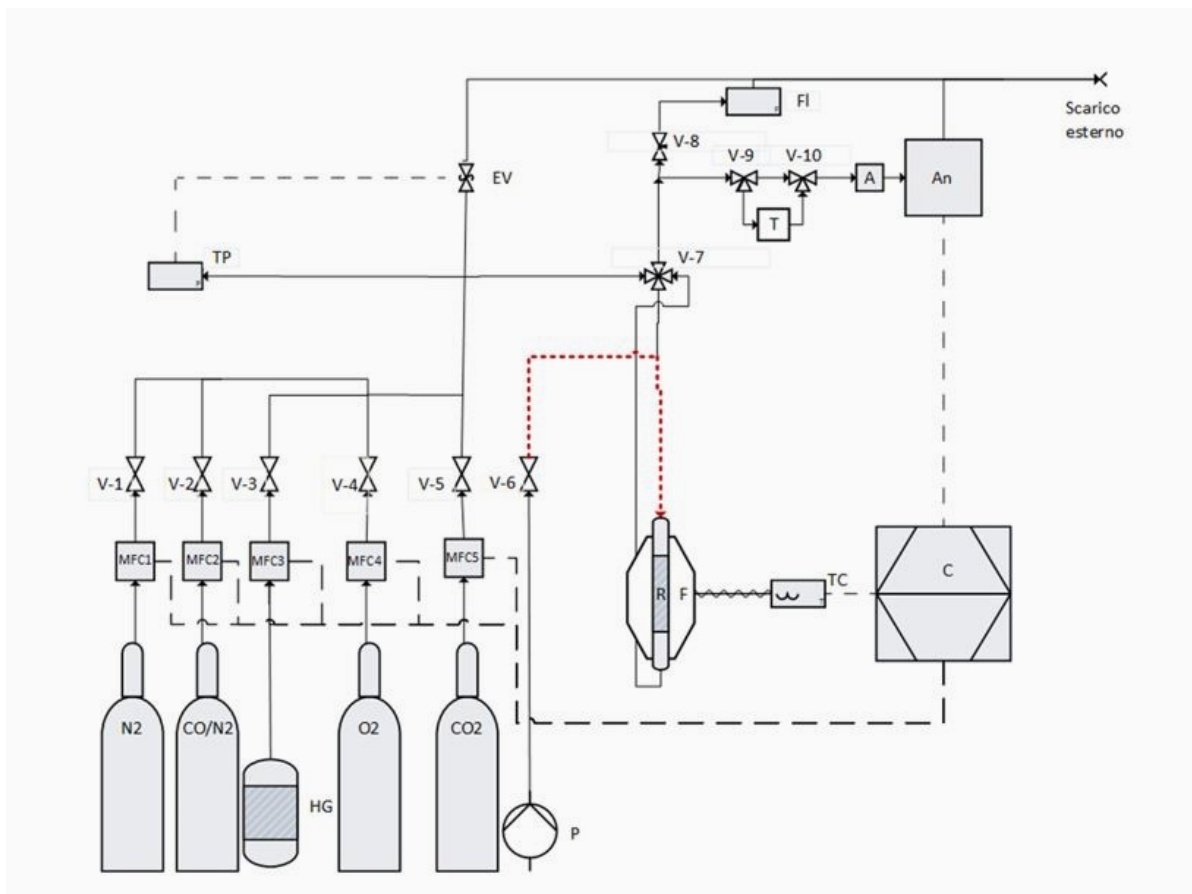


Figure S3. Schematic of the quartz reactor setup.

Table S1. XRD parameters evaluated from the (111) plane: (diffraction angle (2θ , °); cell parameter (a, nm); crystallite size (τ , nm) and specific surface area (SSA, m²/g) of used samples (treated up to 1350 °C).

| Sample | 2θ | a | τ | SSA |
|-----------|-----------|-------|--------|-----|
| CeZr | 28.39 | 0.544 | 23 | 3 |
| Fe-CeZr | 28.18 | 0.548 | 27 | 3 |
| Mn-CeZr | 28.21 | 0.548 | 23 | 3 |
| Cu-CeZr | 28.58 | 0.541 | 24 | 5 |
| K-CeZr | 28.68 | 0.539 | 24 | 4 |
| K-Fe-CeZr | 28.83 | 0.536 | 70 | 4 |
| K-Cu-CeZr | 28.70 | 0.539 | 57 | 5 |

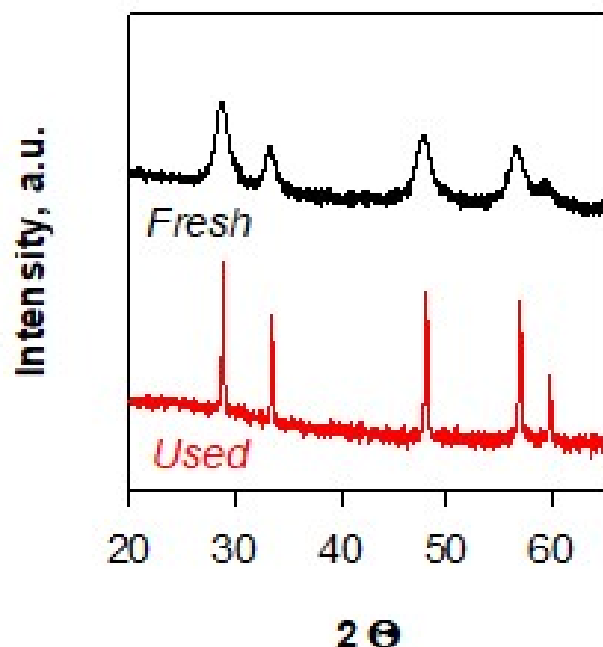


Figure S4. XRD profiles of fresh and used K-Fe-CeZr.

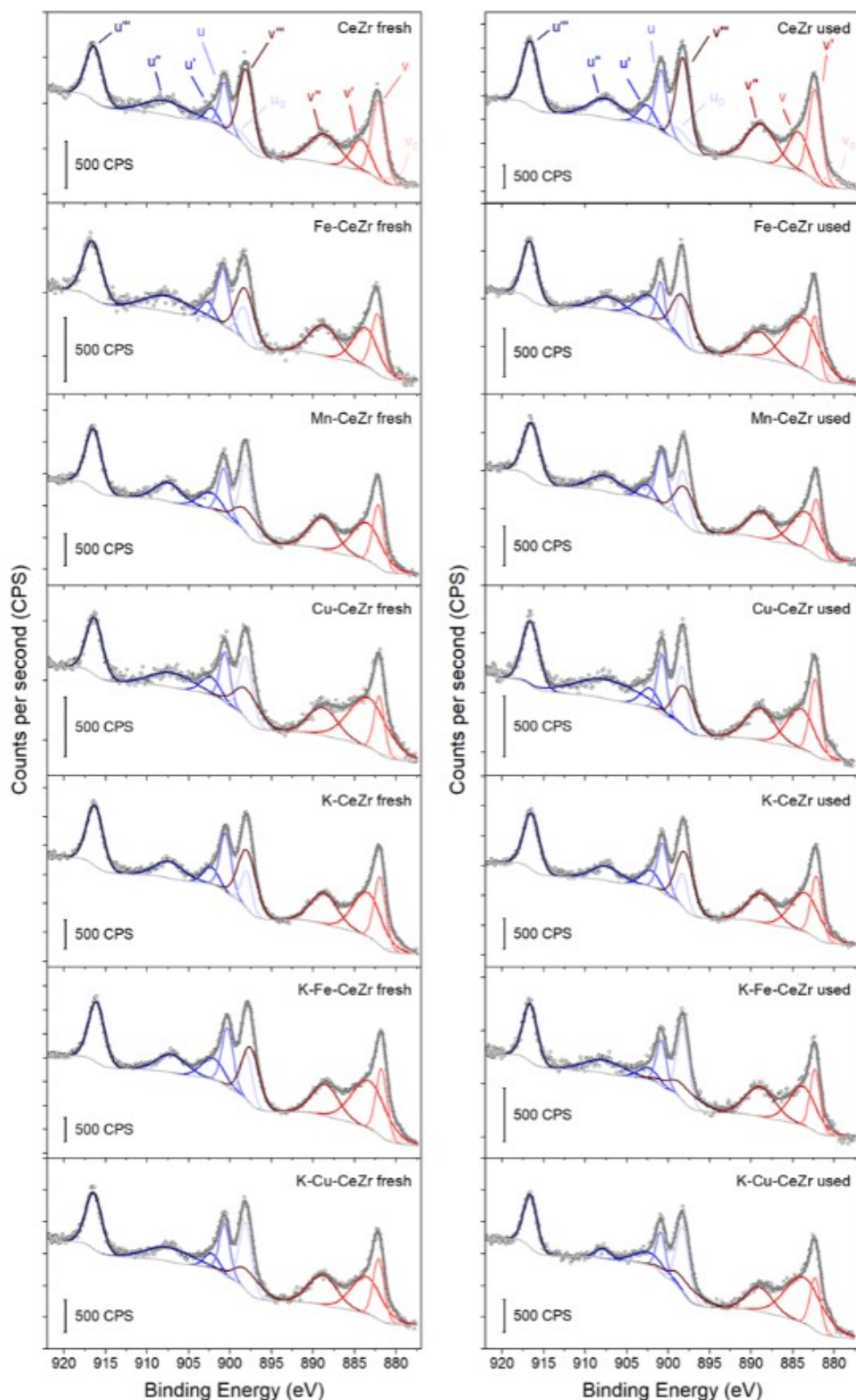


Figure S5. Ce 3d high-resolution XPS spectra with curve-fitting of the fresh (left) and used (right) catalysts.

Table S2. Content of surface labile oxygen (as ratio between labile oxygen (O_α) and bulk oxygen (O_β)) by XPS analysis.

| Sample | Fresh | Used | $\Delta(\text{Ce}/\text{Zr})$ | $\Delta(\text{Ce}^{3+}/\text{Ce}^{4+})$ |
|------------------|--------------------|--------------------|-------------------------------|---|
| | O_α/O_β | O_α/O_β | | |
| CeZr | 1.33 | 0.57 | 0.96 | 0.06 |
| Fe-CeZr | 0.97 | 0.92 | -0.53 | 0.49 |
| Mn-CeZr | 0.92 | 1.42 | -0.92 | -0.15 |
| Cu-CeZr | 1.04 | 1.10 | -1.32 | -0.31 |
| K-CeZr | 0.85 | 0.58 | -0.16 | 0.05 |
| K-Fe-CeZr | 0.67 | 0.68 | -1.76 | 0.03 |
| K-Cu-CeZr | 0.85 | 1.04 | -1.05 | 0.48 |

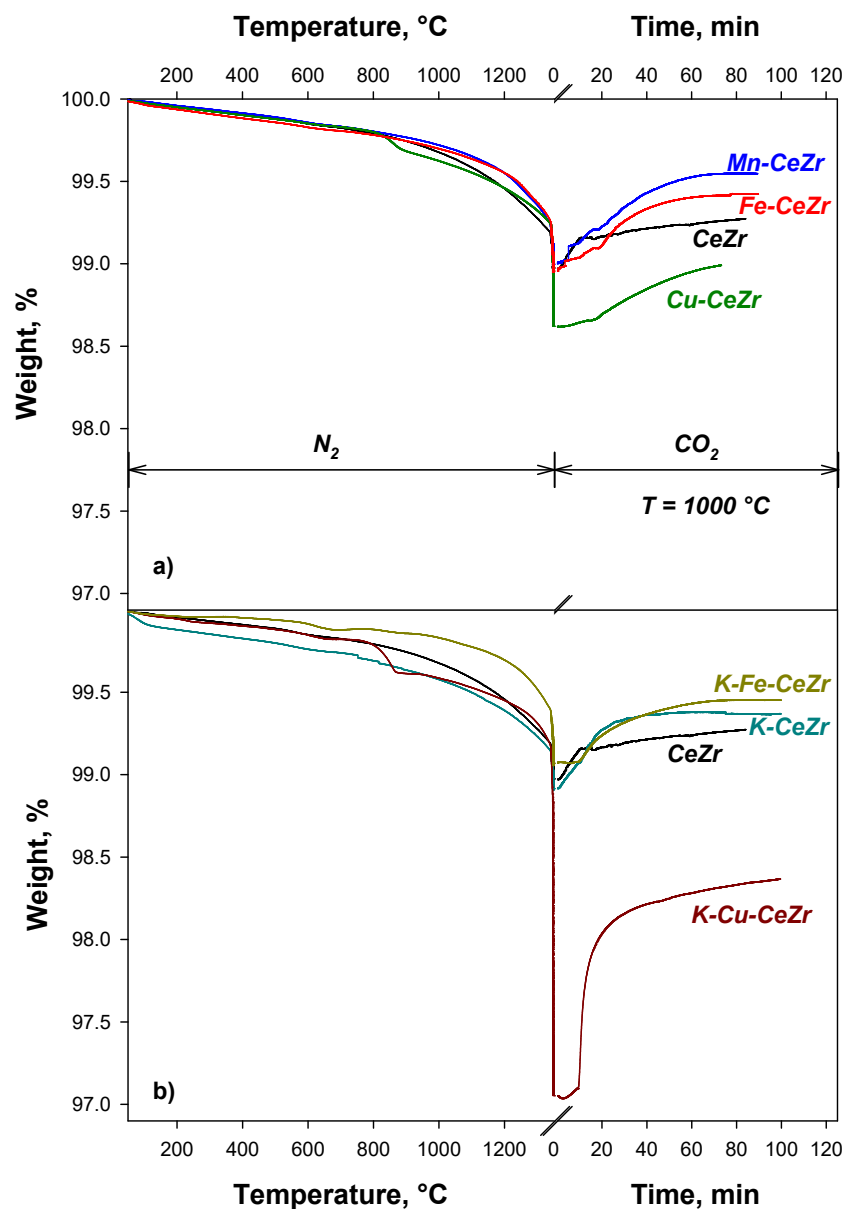


Figure S6. TG profiles of a CO_2 splitting cycle of $\text{M}'\text{-M-CeZr}$ samples. a) undoped and transition metals doped samples; b) undoped and potassium doped and co-doped samples.

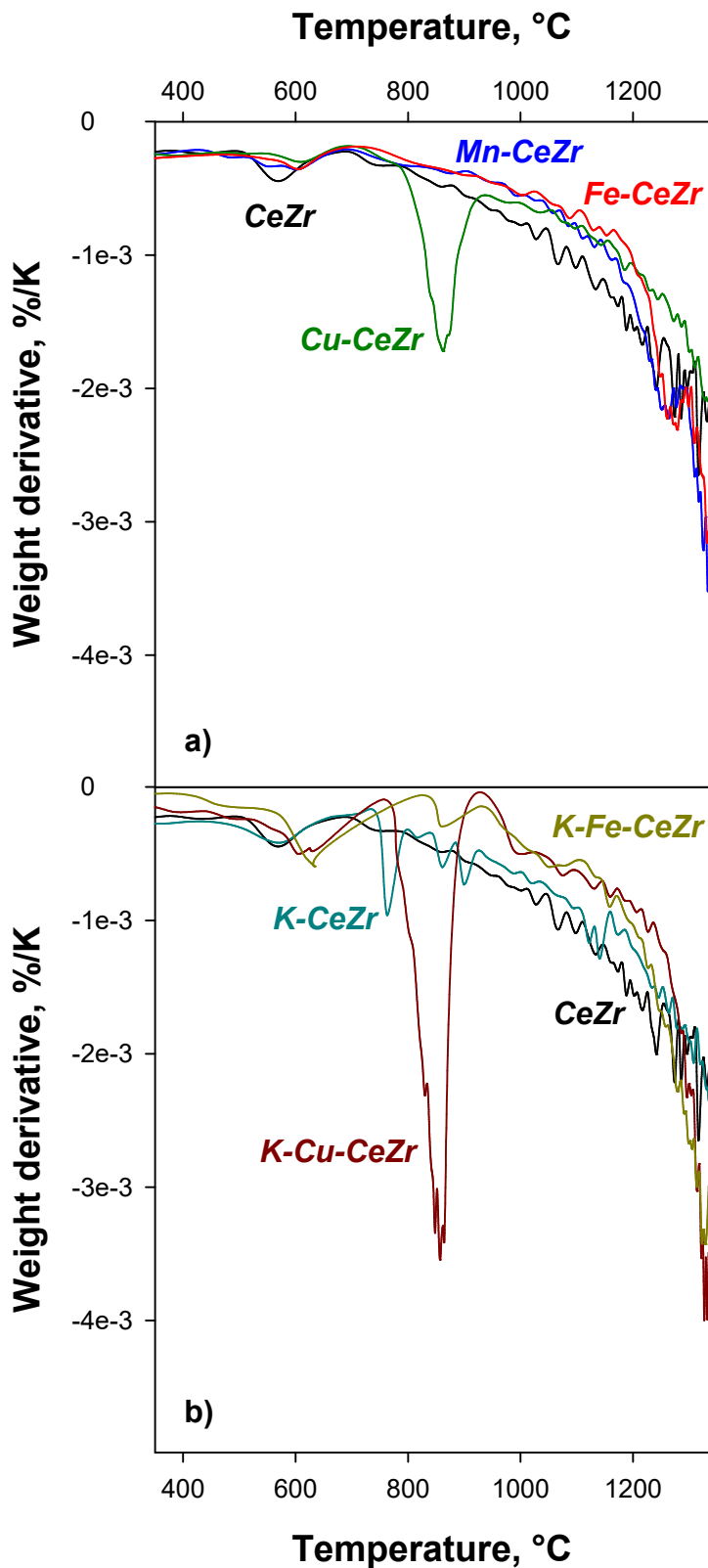


Figure S7. DTG profiles of self-reduction step of the studied samples

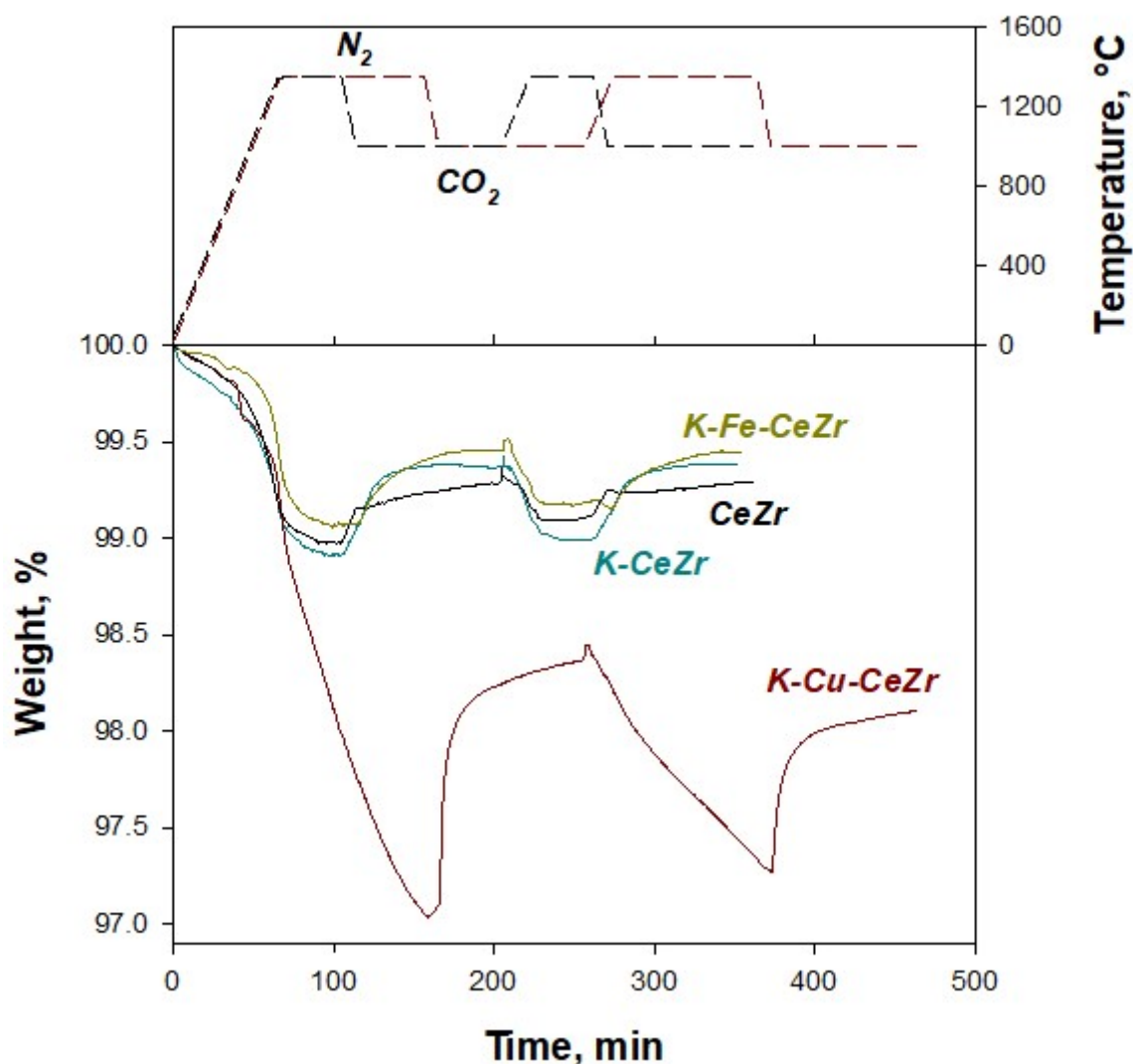


Figure S8. TG profiles of a double CO_2 splitting cycle on bare and K-doped ceria/zirconia samples.

Table S3. . Reduction degree after each step (x_{red} , %), oxidation yield (α , %), and reduction yield (β , %) during thermochemical cycles in TG.

| | | CeZr | Fe-CeZr | Mn-CeZr | Cu-CeZr | K-CeZr | K-Fe-CeZr | K-Cu-CeZr |
|--------------|------------------|-------|---------|---------|---------|--------|-----------|-----------|
| I cycle | x_{red} | 25.6 | 25.6 | 22.9 | 31.4 | 26.6 | 20.5 | 43.1 |
| | β | - | - | - | - | - | - | - |
| | x_{red} | 22 | 16.7 | 13.8 | 26.6 | 12.2 | 9.7 | 30.2 |
| | α | 13.8 | 35 | 39.9 | 15.4 | 54.1 | 52.7 | 29.9 |
| II cycle | x_{red} | 27.4 | - | - | - | 18.4 | 13.1 | 42.8 |
| | β | 151.8 | - | - | - | 43.4 | 31.6 | 97.4 |
| | x_{red} | 26.3 | - | - | - | 11.5 | 8.6 | 40.5 |
| | α | 19.8 | - | - | - | 110.9 | 131.8 | 18.3 |
| III cycle | x_{red} | - | - | - | - | 17.8 | 12.6 | 48.9 |
| | β | - | - | - | - | 91.4 | 88 | 369.5 |
| | x_{red} | - | - | - | - | 12 | 8.9 | 48.2 |
| | α | - | - | - | - | 92.1 | 91.9 | 8.6 |
| IV cycle | x_{red} | - | - | - | - | 18.2 | 12.7 | 53.3 |
| | β | - | - | - | - | 106 | 103.9 | 699 |
| | x_{red} | - | - | - | - | 13.4 | 9.1 | 55 |
| | α | - | - | - | - | 77.3 | 94.7 | 0 |
| V cycle | x_{red} | - | - | - | - | 19.5 | 13.3 | 61.3 |
| | β | - | - | - | - | 127.1 | 116.8 | 0 |
| | x_{red} | - | - | - | - | 14.9 | 10 | 60.9 |
| | α | - | - | - | - | 76.2 | 79.4 | 7.5 |

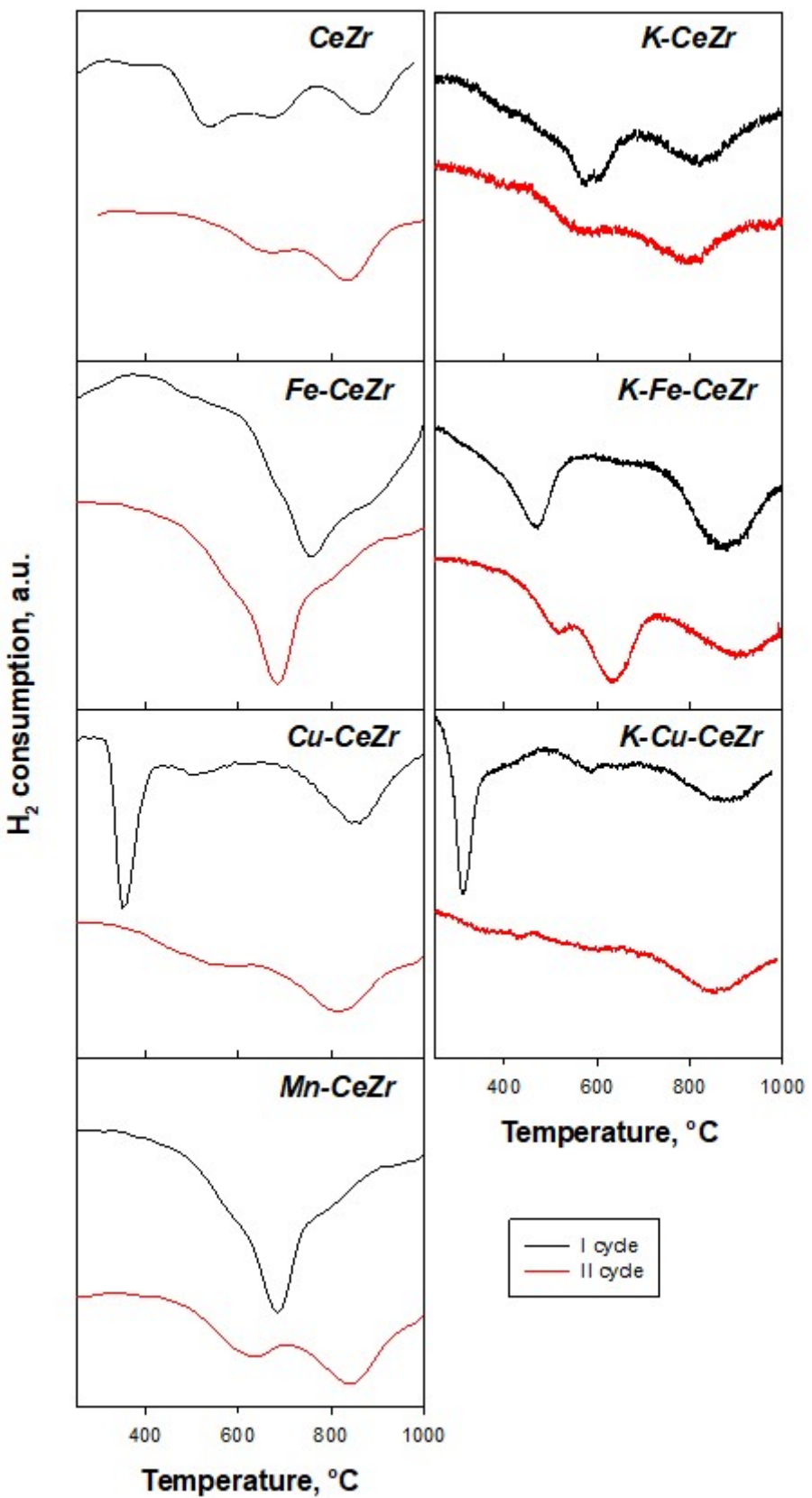


Figure S9. Reduction profiles of the studied samples for two reduction-oxidation cycles.

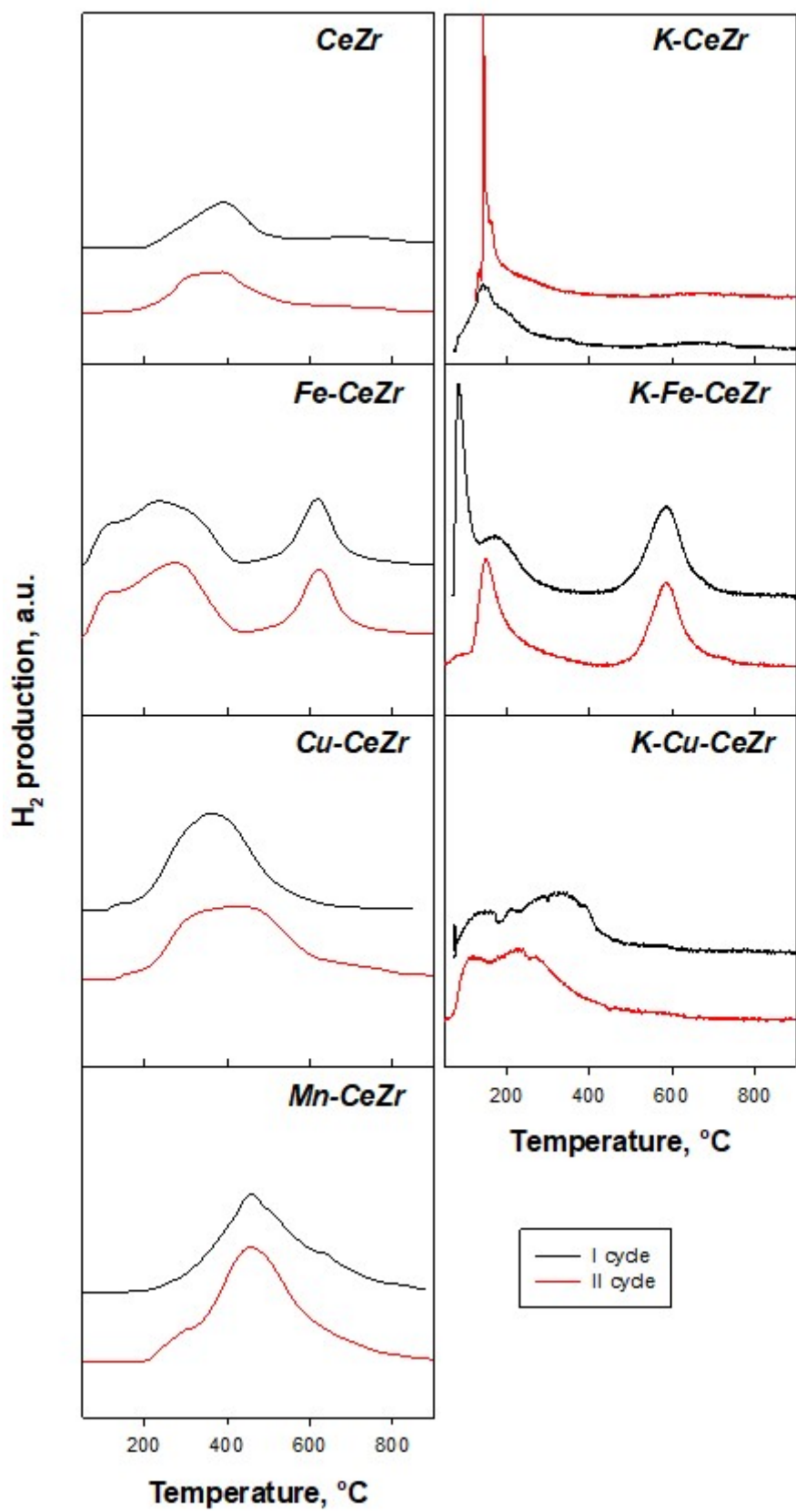


Figure S10. Oxidation profiles of the studied samples for two reduction-oxidation cycles.

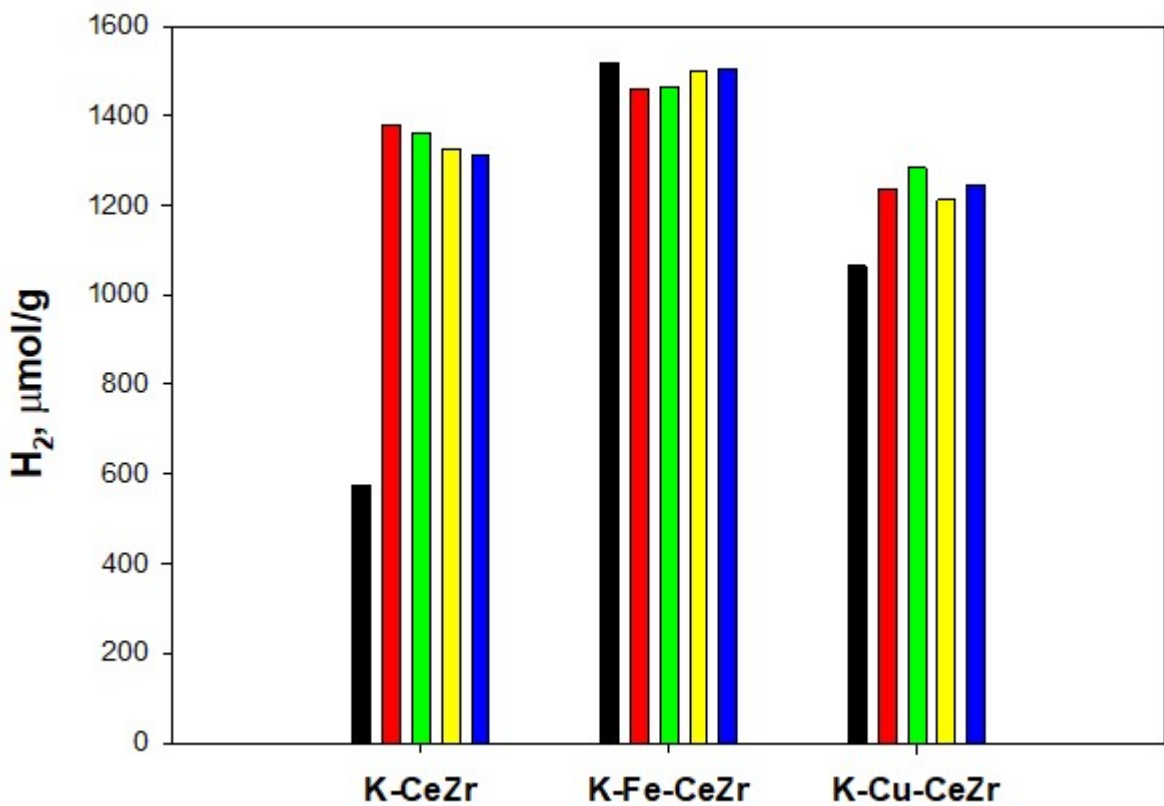


Figure S11. H₂ production during TPO with water of five consecutive TPR/TPO cycles by K containing materials.

Table S4. Reduction degree after each step (x_{red} , %), oxidation yield (α , %), and reduction yield (β , %) during TPR and TPO cycling.

| | Sample | CeZr | Fe-CeZr | Mn-CeZr | Cu-CeZr | K-CeZr | K-Fe-CeZr | K-Cu-CeZr |
|----------|------------------|-------|---------|---------|---------|--------|-----------|-----------|
| I cycle | x_{red} | 36.5 | 63.1 | 66.7 | 60.5 | 44.6 | 49.9 | 78.9 |
| | β | - | - | - | - | - | - | - |
| | x_{red} | 18 | 10.6 | 7.5 | 17.1 | 19.9 | -6.1 | 37.2 |
| | α | 50.9 | 83.1 | 88.8 | 71.8 | 55.5 | 112.2 | 52.8 |
| II cycle | x_{red} | 56.3 | 72.3 | 68 | 61.5 | 67.4 | 49.1 | 81 |
| | β | 206.4 | 117.6 | 102.1 | 102.2 | 191.6 | 98.5 | 105.2 |
| | x_{red} | 34.6 | 20 | 12.9 | 20.2 | 7.7 | -4.8 | 32.6 |
| | α | 56.5 | 84.8 | 91.1 | 92.9 | 125.7 | 97.6 | 110.5 |